Phase-conjugation of the isolated optical vortex using flat surfaces

A. Yu. Okulov

A.M. Prokhorov General Physics Institute of Russian Academy of Sciences, Vavilova Street 38, 119991 Moscow, Russia (alexey.okulov@gmail.com)

Received July 26, 2010; revised September 8, 2010; accepted September 14, 2010; posted September 21, 2010 (Doc. ID 132284); published October 27, 2010

The robust method for obtaining the helical interference pattern due to the phase-conjugation of an isolated optical vortex by means of the non-holographic technique is proposed. It is shown that a perfect wavefront reversal of the vortex in a linear polarization state via an even number of reflections is achievable due to the turn of the photon's momentum $\vec{p} \approx \hbar \vec{k}$ with respect to the photon's orbital angular momentum projection L_z. The possible experimental realization is based on *cat's eye-prism*-like reflections inside the confocal optical *loop* cavity. The alternative scheme contains the Dove prism embedded in the optical *loop* with an odd number of reflections from mirrors. This *confocal* interferometric technique is applicable to optical tweezers, atomic traps, Sagnac laser loops, and metamaterials fabrication.

OCIS codes: 020.7010, 030.6140, 050.4865, 070.5040, 140.3560, 160.1585.

1. INTRODUCTION

Phase-conjugation (PC) proved to be an efficient tool for the laser beam divergence control [1], self-adjustment of optical schemes [2], and beam combination [3] a decades ago. A substantial progress in the understanding of the physical mechanism of a PC mirror is associated with a concept of the phase-singularities inside an optical speckle patterns [4]. In accordance with this concept the randomly spaced dark lines of the speckle [zeros of electric field complex amplitude $\mathbf{E}_f(z,\vec{r}_\perp,t)$] are collocated with the helical phase ramps [5]. Thus the phase-conjugated replica $\mathbf{E}_b(z,\vec{r}_\perp,t)=\mathbf{E}_f^*(z,\vec{r}_\perp,t)$ ought to have a set of its own helical phase ramps collocated with the phase ramps of the incident wave [2]. This helical phase feature of the optical speckle imposes a serious limitation upon the usage of the deformable adaptive mirrors, because the smooth deformable surface is not capable to follow the helical phase ramp. On the other hand the dynamical interference pattern written by the incident speckle and reflected wave inside a nonlinear optical medium, say a stimulated Brillouin scattering (SBS) medium [3] or a photorefractive medium [6], operates like a high-fidelity spatial filter increasing the signal-noise ratio for the backward reflected PC wave $\mathbf{E}_b$.

Recently the concept of phase singularity had been enriched by understanding that helical phase ramps are the sources of the helical interference patterns around zeros of the speckle optical fields [7,8]. In particular it was shown that interference of the two counterpropagating isolated optical vortices in the form of Laguerre–Gaussian (LG) beams produces a helical optical potential or a "lattice with twist" [9]. The key point for achieving such a helical interference pattern proved to be the conservation of the *total* orbital angular momentum (OAM) in a PC mirror: the turn of OAM of a reflected wave is the urgent requirement to the perfect coincidence of the incident and reflected wavefronts and helicoidal interference [8]. It is noteworthy that for the non-PC mirror the OAM is not reversed, and the interference pattern around phase singularity is a toroidal one [10]. The other important feature of the PC mirror is that OAM conservation leads unavoidably to the transfer of rotations to the PC mirror. In the SBS mirror the rotations appear in the form of the helical acoustical phonons with $2\hbar$ OAM; hence optical anisotropy (chirality) emerges in an initially isotropic SBS medium [11]. Quite recently the chiral sound excitations in an initially isotropic liquid were found experimentally and obtained numerically using the Khokhlov–Zabolotskaya–Kuznetsov equation [12]. Nevertheless we will show below that in definite experimental conditions the PC reflection of a single optical vortex with a topological charge ℓ may be achieved experimentally with an even number of reflections from the perfectly flat (nonchiral) surfaces.

2. PROPAGATION OF THE SPECKLE AND ISOLATED VORTEX LINE

The propagation of a speckle field along the *z-axis* means a motion of the field zeros, i.e., the motion of the phase singularities in the same *z-axis* direction. The trajectories of zeros are not rectilinear [11,13,14]; moreover trajectories intertwine each other as it happens with the higher-order LG optical vortex propagation [15]. The intertwining produces the structurally stable twisted entities in a speckle (Fig. 1) as is shown by numerical modeling of the following equation [7]:

$$\frac{\partial \mathbf{E}_{(f,b)}(z,\vec{r}_\perp,t)}{\partial z}+\frac{n(z,\vec{r}_\perp)}{c}\frac{\partial \mathbf{E}_{(f,b)}}{\partial t}\pm\frac{i}{2k_{(f,b)}}\Delta_\perp \mathbf{E}_{(f,b)}=0, \quad (1)$$

where $n(z,\vec{r}_\perp)$ is the inhomogeneity of the refractive index, and $k_{(f,b)}=|\vec{k}_{f,b}|\approx k_z$ are the wave numbers of the counterdirected incident and reflected speckle fields, with

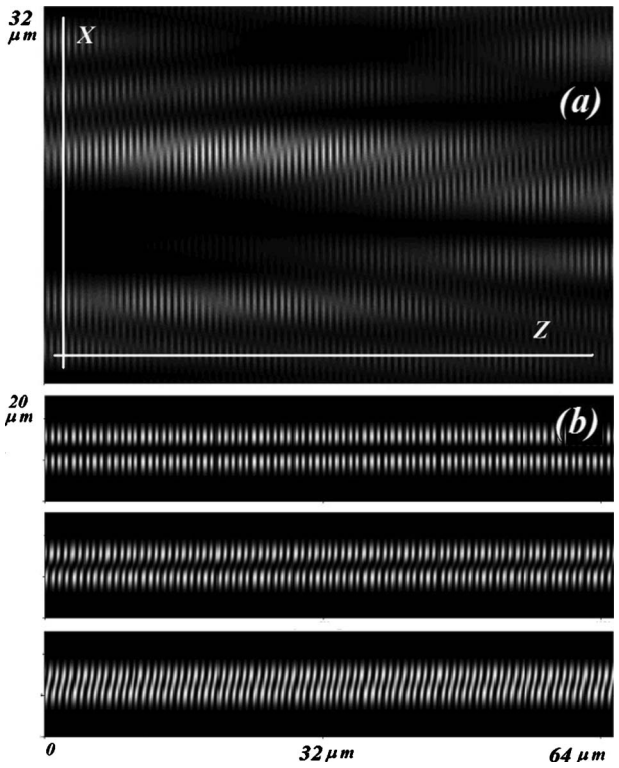

Fig. 1. (a) Intertwining of the helical interference patterns in the optical speckle [7]. The size of pattern is 32 μm in X-direction and 64 μm in Z-direction. The period of longitudinal (Z) modulation is $\lambda/2$. (b) In contrast to optical vortices in a speckle the isolated LG optical vortices propagate rectilinearly. Interference pattern (4) is sliced at $Y=0,5,10$ μm distances from the vortex axis Z.

boundary condition as a multimode random field [16] composed of N_g plane waves having amplitudes $A_{j_x j_y}$, random phases $\theta_{j_x j_y}$, and randomly tilted wave vectors, each having random transverse projections $\vec{k}^{\perp}_{jx,jy}$ at the $z=0$ plane:

$$\mathbf{E}_{(f)}(\vec{r},0) \approx \mathbf{E}^0_{(f)} \sum_{j_x j_y \in N_g} A_{j_x j_y} \exp[i\vec{k}^{\perp}_{j_x j_y} \cdot \vec{r}_{\perp} + i\theta_{j_x j_y}]. \quad (2)$$

The paraxial propagation [17] of the randomly tilted plane waves produces the twisted interference patterns resembling visually the *ropes*, each composed of several intertwined optical vortices [7,15]. The similar propagation behavior and appearance of the *knot* structures had been reported in [13,14].

In contrast to the speckle field, the isolated vortex line propagates rectilinearly in a free space, and it is structurally stable (Fig. 1). This happens, for example, for the LG-laser beam with a topological charge ℓ [18]:

$$\mathbf{E}_{(f,b)}(z,r,\theta,t) \sim \frac{\mathbf{E}^0_{(f,b)} \exp[i(-\omega_{(f,b)}t \pm k_{(f,b)}z) \pm i\ell\theta]}{(1+iz/(k_{(f,b)}D_0^2))^2}(r/D_0)^{\ell} \times \exp\left[-\frac{r^2}{D_0^2(1+iz/(k_{(f,b)}D_0^2))}\right], \quad (3)$$

where $[(z,r,\theta,t) \rightarrow (z,\vec{r}_{\perp},t)]$ are cylindrical coordinates embedded at the LG axis (z-*axis*). This straight vortex line is the exact self-similar solution of the free-space

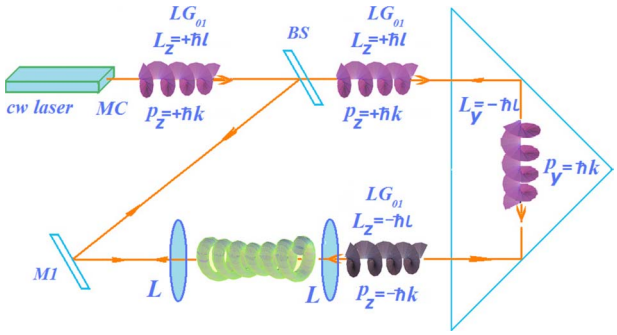

Fig. 2. (Color online) Two consecutive reflections of LG beam emitted by continuous-wave laser with mode converter MC. Each total internal reflection inside the *cat's eye* prism from plane prism surface changes the topological charge of LG ℓ to the opposite one. After two reflections at 45° angle the optical vortex has the opposite direction of propagation and opposite direction of the angular momentum. The counterpropagating LG has the same topological charge ℓ; hence composite wavetrain produces the helical interference pattern. Confocal telescope consisting of the thin lenses L compensates the free-space propagation parabolic wavefront.

wave equation in a paraxial approximation (1). Our aim is to describe how to use the structural stability and hence self-similar propagation of the optical vortex for the nonholographic wavefront reversal by conventional mirrors, lenses, and prisms. At first sight our proposal looks like a counterintuitive one, because we focus the attention of experimentalists upon previously criticized *cat's eye* prism PC techniques [2]. The case is that the *ray reversal* (with small lateral displacement) inside the prism is not able to perform a *wave propagation* reversal of the random collection of optical vortices in a speckle field or in the complicated image optical field. This seeming paradox is resolved by taking into account that ray reversal means a photon's *momentum* reversal, while helical phase singularity is reversed by means of the *angular momentum* reversal [8]. It is noteworthy that the OAM direction is changed to the opposite one inside a Dove prism due to one total internal reflection inside the prism (at 45° incidence angle) and two refractions [19]. The same happens in *cat's eye* prism due to the same reason: when the plane surface is tilted at the angle α with respect to the propagation of vortex, the rotational symmetry of the setup is absent; hence the angular momentum is not conserved, and the OAM is rotated at a 2α angle. For both prisms the

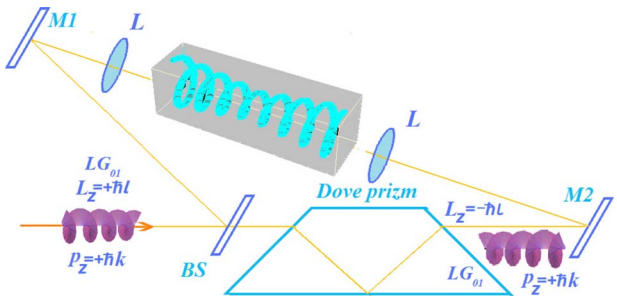

Fig. 3. (Color online) Single reflection inside Dove prism changes the topological charge. After the two refractions the LG propagates with conserved momentum and overturned angular momentum. This leads to helical interference pattern due to overlapping with counterpropagating LG, having opposite OAMs.

change in the angular momentum is $2\hbar$ per photon; hence the prisms feel the torque $|\vec{T}|=2I/\omega$, where I is the intensity and ω is the radiation frequency [8]. As a consequence of the OAM reversal the vortex propagates in the optical *loop* schemes (Figs. 2 and 3) as a perfectly phase-conjugated one due to the simple reflections from conventional prism surfaces, provided the vortex is slightly focused by a thin lenses in order to compensate diffractive divergence. The technical requirements for the *loop* adjustment are the same as those previously formulated for the ring lasers and Fabry–Perot cavities with Hermite–Gaussian and LG beams [10].

3. ANGULAR MOMENTA ORIENTATION AND ROTATION OF INTERFERENCE PATTERN

Let us assume the ultimate quality of a PC reflection of the linearly polarized ($\mathbf{E}^0_{(f,b)}\|\mathbf{y}$-axis) ℓth order LG-laser beam. Then the interference pattern inside the beam waist reads as

$$|\mathbf{E}_f(z,r,\theta,t)+\mathbf{E}_b(z,r,\theta,t)|^2 \sim |\mathbf{E}^0_{(f,b)}|^2(r/D_0)^{2\ell}\exp\left[-\frac{2r^2}{D_0^2(1+iz/(k_{(f,b)}D_0^2))}\right] \times[1+\cos[(\omega_f-\omega_b)t-(k_f+k_b)z+2\ell\theta]]. \quad (4)$$

The helicity of pattern is due to the self-similar phase argument $(\omega_f-\omega_b)t-(k_f+k_b)z+2\ell\theta$ which remains a constant at the double helix with a diameter $\sim 2D_0$ and $\lambda/2$ pitch ($\lambda=2\pi/k_{(f,b)}$) [8]. Such a double helix optical potential rotates with angular frequency $\Omega=\omega_f-\omega_b$ which looks attractive from the point of view of optical microfluidics, micro- and nano-particle manipulation [6,15], and as an optical dipole trap for ultracold atomic ensemble [9].

The key point in the physical interpretation of this helical pattern is the mutual orientation of the photon momentum $\vec{p}\approx\hbar\vec{k}$ and the projection of the photon OAM L_z on the propagation axis [8,18]. The mutual orientation of both quantum and classical momenta $\vec{p}$ and angular momenta $\vec{L}$ is changed after single reflection from an isotropic optical element, namely, a metal or a multilayer dielectric mirror. On the contrary the anisotropic structures inside a wavefront reversal mirror [8] perform turn of the OAM of the laser beam because of the wavefront matching property of PC-mirror. This turn operation is analogous to the photon spin turn (change of the circular polarization to the oppositely rotating one) when passing through a birefringent plate (i.e., an anisotropic crystal) [20].

Consider two optical *loop* schemes (Figs. 2 and 3) composed of plane mirrors, ideal thin lenses for adjusting of the parabolic component of the wavefronts (3) [19], and prisms (possibly with a laser gain medium inside). As is shown in [8] each reflection from the plane mirror changes the mutual orientation of the photon momentum $\hbar\vec{k}_z$ and the angular momentum $L_z=\pm\hbar\ell\vec{z}/z$ to the opposite one.

Consequently two reflections in Fig. 2 scheme do not change the topological charge of photon, and the oppositely propagating wave possesses the helical wavefront with the same handedness. Thus the LG beam reflected inside *cat's eye* prism and the other LG beam reflected from the beam splitter BS and mirror M1 will have the perfect wavefront coincidence, provided their parabolic phase profiles that occur due to a free-space propagation are compensated by a thin lens (Figs. 2 and 3). As a result the interference pattern will have a double helix geometry, provided their path difference is smaller than the coherence length $\Delta l_{\mathrm{coh}}=c\tau$ (τ is the coherence time). Alternatively in Fig. 3 scheme the *single* reflection inside the Dove prism changes the topological charge of each photon to the opposite one [19], and the else reflection from mirror M2 is needed to restore the mutual orientation of the OAM and momentum. This sequence of reflections ensures the helical wavefront coincidence and produces the helical interference pattern with the twice-reflected (BS +M1) counterpropagating LG beam. The removal of the Dove prism will produce a toroidal interference pattern because of the absence of PC and parallel orbital angular momenta of colliding photons [6,8,10].

The frequency shift Ω may be produced via two different mechanisms. The first mechanism is the rotational Doppler shift which arises because of rotation of the birefringent half-wavelength plate, which alternates the spin component of angular momentum [15,21], or the rotating Dove prism, which alternates the orbital component of angular momentum [22]. The Dove prism rotation technique is difficult to implement because of strict alignment requirements for interference pattern control. The other mechanism is the Sagnac frequency shift which appears in a ring laser located in the rotating reference frame. This might happen when prisms have laser gain areas collocated with the LG beam propagation. Typically the optical gain is induced in a rare-earth doped dielectric host crystals by virtue of the diode laser pump [23]. In this case the external laser outside the *loop* is not necessary, and the beam splitter BS is to be replaced to return mirror R3. The conditions for the selection of a given transverse LG mode are to be fulfilled [24], and such a case deserves special consideration elsewhere. As is well known for the *loop* laser schemes the counterpropagating beams have different frequencies ω_f and ω_b because of the Earth rotation having angular frequency $\Omega_\oplus$ and the angular frequency of the optical table rotation Ω_{lab}. For such *Sagnac loop* [24] the frequency splitting is

$$\Omega=(\omega_f-\omega_b)=\frac{16\pi^2A\Omega_r}{P\lambda}, \quad (5)$$

where $\Omega_r=\Omega_\oplus+\Omega_{\mathrm{lab}}\sim(2\pi/86,400)+\Omega_{\mathrm{lab}}$ is the angular speed of rotation of the laboratory frame, and P and A are the perimeter and the square of the loop, respectively. The frequency shift is measured by a detection of beats (rotation of the interference pattern in our case) of the counterpropagating intracavity beams behind the cavity mirrors (M1 and M2 in Figs. 2 and 3). For the typical ratio of the spatial dimensions of the *Sagnac loop laser* to the wavelength $\lambda\sim 1$ μm, the frequency splitting proves to be $\Omega\approx 2\pi\times 10^{-(1-3)}$ rad/s. In particular the evaluation of Ω is straightforward for the circular ring cavity of radius R

when $P=2\pi R$, $A=\pi R^2$: the frequency splitting is $\Omega=\Omega_r 8\pi^2 R/\lambda$.

4. CONCLUSION

In summary we proposed the phase-conjugation (PC) of an isolated optical vortex line (LG beam) with lateral displacement in the confocal optical *loop* scheme with an *even* number of reflections. The alternative optical loop with an *odd* number of mirrors contains a Dove prism that alternates the photon OAM projection after the straight passage through a prism. This scheme is different from the Mach–Zehnder setup used previously for rotational Doppler effect study [15,21,22]. Our loop setups with colliding phase-conjugated optical vortices and helical interference patterns herein are promising tools for nonexpensive replacement of nonlinear optical phase conjugators based on SBS [2,3], photorefractive crystals [6], and liquid crystal light valves. The field of experimental applications of confocal loops with cat's eye prism or Dove prism is in atomic traps [9] and optical tweezers, in particular in assembling protein-like clusters [25]. The other intriguing application is in the lithography of metamaterials [26,27] and optical waveguides with helical refractive indices and conductivities [28].

REFERENCES

1. R. Hellwarth, "Generation of time-reversed wave fronts by nonlinear refraction," J. Opt. Soc. Am. **67**, 1–3 (1977).
2. B. Y. Zeldovich, N. F. Pilipetsky, and V. V. Shkunov, *Principles of Phase Conjugation* (Springer-Verlag, 1985).
3. N. G. Basov, I. G. Zubarev, A. B. Mironov, S. I. Mikhailov, and A. Y. Okulov, "Laser interferometer with wavefront reversing mirrors," Sov. Phys. JETP **52**, 847–851 (1980).
4. J. F. Nye and M. V. Berry, "Dislocations in wave trains," Proc. R. Soc. London, Ser. A **336**, 165–190 (1974).
5. I. Basistiy, M. S. Soskin, and M. V. Vasnetsov, "Optical wave-front dislocations and their properties," Opt. Commun. **119**, 604–612 (1995).
6. M. Woerdemann, C. Alpmann, and C. Denz, "Self-pumped phase conjugation of light beams carrying orbital angular momentum," Opt. Express **17**, 22791–22799 (2009).
7. A. Yu. Okulov, "Twisted speckle entities inside wavefront reversal mirrors," Phys. Rev. A **80**, 013837 (2009).
8. A. Yu. Okulov, "Angular momentum of photons and phase conjugation," J. Phys. B **41**, 101001 (2008).
9. M. Bhattacharya, "Lattice with a twist: Helical waveguides for ultracold matter," Opt. Commun. **279**, 219–222 (2007).
10. T. Puppe, I. Schuster, A. Grothe, A. Kubanek, K. Murr, P. W. H. Pinkse, and G. Rempe, "Trapping and observing single atoms in a blue-detuned intracavity dipole trap," Phys. Rev. Lett. **99**, 013002 (2007).
11. A. Yu. Okulov, "Optical and sound helical structures in a Mandelstamm–Brillouin mirrors," JETP Lett. **88**, 487–491 (2008).
12. R. Marchiano, F. Coulouvrat, L. Gnjehi, and J.-L. Thomas, "Numerical investigation of the properties of nonlinear acoustical vortices through weakly heterogeneous media," Phys. Rev. E **77**, 016605 (2008).
13. J. Leach, M. R. Dennis, J. Courtial, and M. J. Padgett, "Vortex knots in light," New J. Phys. **7**, 55 (2005).
14. M. R. Dennis, R. P. King, B. Jack, K. O'Holleran, and M. J. Padgett, "Isolated optical vortex knots," Nat. Phys. **6**, 118–121 (2010).
15. M. P. MacDonald, K. Volke-Sepulveda, L. Paterson, J. Arlt, W. Sibbett, and K. Dholakia, "Revolving interference patterns for the rotation of optically trapped particles," Opt. Commun. **201**, 21–28 (2002).
16. A. Yu. Okulov, "The effect of roughness of optical elements on the transverse structure of alight field in a nonlinear Talbot cavity," J. Mod. Opt. **38**, 1887–1890 (1991).
17. A. Yu. Okulov, "Two-dimensional periodic structures in nonlinear resonator," J. Opt. Soc. Am. B **7**, 1045–1050 (1990).
18. L. Allen, M. W. Beijersbergen, R. J. C. Spreeuw, and J. P. Woerdman, "Orbital angular momentum of light and the transformation of Laguerre–Gaussian laser modes," Phys. Rev. A **45**, 8185–8189 (1992).
19. J. Leach, M. J. Padgett, S. M. Barnett, S. Franke-Arnold, and J. Courtial, "Measuring the orbital angular momentum of a single photon," Phys. Rev. Lett. **88**, 257901 (2002).
20. R. A. Beth, "Mechanical detection and measurement of the angular momentum of light," Phys. Rev. **50**, 115–125 (1936).
21. J. Arlt, M. MacDonald, L. Paterson, W. Sibbett, K. Volke-Sepulveda, and K. Dholakia, "Moving interference patterns created using the angular Doppler-effect," Opt. Express **10**, 844–852 (2002).
22. Ch. V. Felde, P. V. Polyanski, and H. V. Bogatyryova, "Comparative analysis of techniques for diagnostics of phase singularities," Ukr. J. Phys. Opt. **9**, 82–90 (2008).
23. A. Yu. Okulov, "Scaling of diode-array-pumped solid-state lasers via self-imaging," Opt. Commun. **99**, 350–354 (1993).
24. M. O. Scully and M. S. Zubairy, *Quantum Optics* (Cambridge U. Press, 1997), Chaps. 4 and 17.
25. D. Zerrouki, J. Baudry, D. Pine, P. Chaikin, and J. Bibette, "Chiral colloidal clusters," Nature **455**, 380–382 (2008).
26. V. G. Veselago, "The electrodynamics of substances with simultaneously negative values of ϵ and μ," Sov. Phys. Usp. **10**, 509–514 (1968).
27. M. Thiel, H. Fischer, G. von Freymann, and M. Wegener, "Three-dimensional chiral photonic superlattices," Opt. Lett. **35**, 166–168 (2010).
28. Z. Menachem and M. Mond, "Infrared wave propagation in a helical waveguide with inhomogeneous cross section and application," PIER **61**, 159–162 (2006).